Magnetic Resonance Imaging Reconstruction Based on Dynamic Threshold Shrinkage of Low-Rank Matrix

Boyu Tao [a], Jianghang Long [b]

College of Electronic Engineering, Chongqing University of Posts and Telecommunications, Chongqing 400065, China.

[a]saginardo@163.com, [b]3538108138@qq.om

Abstract

The global fixed sparse basis can not reflect the sparse features of the magnetic resonance(MR) image well, which may cause the reconstructed MR images suffer from the problem of losing details and textures. To improve the quailty of reconstructed MR images, a new algorithm is proposed by using low-rank matrix dictionary, which is constructed based on the non-local similar sub-image blocks. Besides, this algorithm introduces a dynamic threshold shrinkage method aiming at solving the low rank problems more effective. The method is to explore the non-local similarity of MR images to further enhance the quality of reconstructed images. Experiment results show that the proposed method improves the peak signal-to-noise ratio, structural similarity index and subjective vision of the reconstructed image.

Keywords

MR Image Reconstruction, Compressed Sensing, Low-Rank Matrix Dictionary, Nonlocal Similarity.

1. Introduction

Magnetic resonance imaging (MRI) is a technology to capture different structures of different materials in the presence of strong magnetic field and gradient magnetic field[1]. MRI has many advantages, such as no invasion, no ionizing radiation and accurate image reconstruction. Nowadays, this technology has become an important imaging method, which is greatly promoted the rapid development of modern clinical medicine, neurophysiology and profile diagnosis technology. However, MRI has a obvious disadvantage, namely is the slow imaging speed limited by slow data acquisition speed and many phase encoding in one acquistion time, which would caused a long imaging time. There are many methods proposed to solve this slow imaging issue, such as Rapid Acquisition with Relaxation Sequence[2], Gradient Recalled Echo Sequence[3], multi-channel parallel imaging technology[4]. These method require high performance hardware, but since the compressed sensing(CS) Theory was proposed, MRI reconstruction becomes more efficient and accurate with little improve of hardware[5].

The application of the compressed sensing theory in MRI is due to the characteristics of the magnetic resonance signal itself. Firstly, the information complexity of MRI is not as high as that of natural images. Most MRI signals have good sparsity in the spatial domain or in some specific domains. For example, magnetic resonance angiography itself is sparse in spatial domain, and vascular tissue imaging can further reduce data sampling by finite difference. Brain imaging has piecewise smooth characteristics, and it shows better sparsity in total variation sparse domain. Secondly, the distribution of spatial magnetic resonance signals have the following characteristics: a large number of low-frequency information is distributed in the central area of k-space, which determines the overall structure of the image. A small amount of high-frequency information is distributed around the k-space, which determines the detail texture characteristics of the image. The spatial characteristics of sparse separation make the design of observation matrix more easier, which can be designed for dense sampling of spatial center data and sparse sampling for non central area, and such sampling mode can also well satisfy the RIP condition[7].

Considering the factors such as measurement error or noise interference in practical application, the equation of MRI reconstruction based on compressed sensing can be expressed as:

$$\arg\min \|\Psi\rho\|_P \quad s.t. \quad \|F_u\rho - d\|_2^2 < \varepsilon \tag{1}$$

Where ρ is the original image, Ψ is a sparse transformation, such as the usual wavelet transform. F_u is the under-sampling matrix, and d is the measured result in k-space. $\|\bullet\|_P$ is a norm constraints determined by specific function, such as l_1 norm constraints or TV norm constraints. The ε is the error between measuring data and real data, which is usually caused by noise interference or coil jitter and so on. The constraints mentioned above can be transformed into unconstrained optimization problems by converting to regularization terms:

$$\arg\min \|F_u\rho - d\|_2^2 + \lambda\|\Psi\rho\| \tag{2}$$

where $\|\Psi\rho\|$ is a given regularization norm. There are many methods tring to solve the above equation, such as TV-weighted algorithm[8], refrence image guided algorithm[9], bayes formula[10] and so on. But these methods are based on the global fixed sparse basis function, thus may lead losing details and textures for MR images. To the bese of our knowlegde, this work represents a low-rank based method with the CS theory to reconstruct the MR Image effictively.

2. Nonlocal Low-Rank Matrix Regularization

2.1 Nonlocal Similarity

The MR image itself has strong structural characteristics, which means that the selected sub-image block may be similar with any other sub-image blocks. In another word, if one signle image block is selected from the MR image, many other highly similar sub-image blocks can be found and mathed in the entire image. These blocks are distributed in different regions of the image, and this similarity between these blocks is called nonlocal similarity[11]. The matrix dictionary, which is composed of similar blocks in MR images, can be regarded as an overcomplete sparse base of the image.

For a selected pixel i in an image u, the nonlocal method is used to estimate the pixel value by all matched sub-image blocks based on weighted average mean:

$$NLM(u(i)) = \sum w(i,j)u(j),\ j \in \Omega \tag{3}$$

where, $NLM(u(i))$ is the estimate value of the pixel i, Ω is the set of all matched sub-image blocks, and $w(i,j)$ is the weighted parameter for every match pixel j, which is restricted by the following equation:

$$\sum_j w(i,j)=1\ ,\ 0 \le w(i,j)_j \le 1 \tag{4}$$

This weighted parameter $w(i,j)$ can be caculated by the gauss weighted euclidean distance as follows:

$$w(i,j) = \frac{1}{Z(i)} e^{-\frac{D(i,j)}{h^2}} \tag{5}$$

where $D(i,j)$ is the eucliden distance of sub-image blocks as in equation (6), and $Z(i)$ is a normalization onstant as in equation (7), namely:

$$w(i,j)=\frac{1}{Z(i)}e^{-\frac{D(i,j)}{h^2}} \tag{6}$$

$$Z(i)=\sum_i e^{-\frac{D(i,j)}{h^2}} \tag{7}$$

2.2 Low-Rank Constraint Regularization

The matrix formed by a set of nonlocal sub-image blocks reflects the correlation between the selected sub-image block and other similar sub-image blocks in the observation window. and this low-rank matrix contains a lot of redundant information. The matrix formed by similar sub-image blocks, which are stretched into column vectors, constitute coherence between column vectors, so such a low-rank matrix can be used as a sparse prior information needed for compressed sensing theory, which can effectively reconstruct magnetic resonance signals.

Low-rank matrices are often subject to noise or error interference in practice, such a solution to low-rank matrix can be expressed as:

$$Y=X+E \tag{8}$$

where $Y\in C^{m\times n}$ is the observed result, $X\in R^{m\times n}$ is a low-rank matrix , $E\in R^{m\times n}$ is an unknown noise matrix. Equation (9) describes the problem of how to find an approximation of the lowest rank matrix X with a known observation matrix Y , and such an optimization problem can be expressed as:

$$\min_{X\in C} rank(X)\ s.t.\ \|X-Y\|_F^2\le\varepsilon \tag{9}$$

where $rank(X)$ is the rank of matrix X , ε is an error value, and $\|\bullet\|_F^2$ represents the Frobeniu norm. The solution of equation (10) is a NP-hard problem, which belongs to the non convex optimization problem, and there is no direct solution at the present stage. In [12], it has been proved that nuclear norm minimization can be used to solve the low-rank constraint problems, in which nuclear norm is defined as the sum of all singular values of a matrix as:

$$\|X\|_*=\sum_i \sigma_i(X) \tag{10}$$

Thus, the equation (10) can be turned to unconstrained optimization problems and can be solved by the nuclear norm, namely:

$$\arg\min_{X\in C}\|X-Y\|_F^2+\lambda\|X\|_* \tag{11}$$

where λ is the regularization parameter.

3. Optimization Algorithm for MRI Reconstruction

As discussed in above chapter, image non-local similarity reflects the sparse structure of the image itself. The traditional low-rank constraint reconstruction method aims to reconstruct the minimum low-rank residual and reconstruct the image to a certain extent, which will ignore the details of the image. Therefore, in this section, a dynamic threshold shrinkage MR image reconstruction method is proposed based on low-rank matrix constraint from the perspective of improving the solution of low-rank matrix. The experiment results show that this method has advantages in maintaining the texture details.

Firstly, $\rho\in C^{N\times M}$ is a MR image with $N\times M$ resolution size, $F_u\in C^{u\times P}$ represents the fourier undersampling matrix, d represents the sampling result, and the reconstructed target is to recover the original matrix from the undersampling results:

$$d=F_u\rho \tag{12}$$

Take $R_i \in C^{n\times p}$ as the extraction matrix, then the i-th sub-image block can be described as:

$$R_i\rho=[R_{i1}\rho, R_{i2}\rho, R_{i3}\rho, ..., R_{im}\rho] \in C^{n\times m}, n \le m \tag{13}$$

where n is the length of the column vector of a sub-image block, and m is the volume of similar sub-image blocks, and ρ_{i1} is one of the low-rank matrix related to the selected block, so the low-rank constraint can be explained as:

$$L_i = \arg\min_{L_i} rank(L_i) \;\; s.t. \;\; \|R_i\rho - L_i\|_F^2 \le \sigma_w^2 \tag{14}$$

According to the low-rank property of similar matrix, the low rank matrix is minimized as the constraint term, and a magnetic resonance reconstruction method based on nonlocal low-rank matrix constraint is presented:

$$\arg\min_{\rho} \|F_u\rho - d\|_2^2 + \eta\sum_i \{\|L_i\|_* + \lambda\|R_i\rho - L_i\|_F^2\} \tag{15}$$

where this equation can be decomposited into subproblems with closed solutions by the alternate multiplier method:

$$\omega_i^{t+1} = \arg\min_{\omega, L_i} \beta\left\|\rho^t - \omega^t + m^t\right\|_2^2 + \eta\sum_i \left\{\|L_i\|_* + \lambda\|R_i\rho - L_i\|_F^2\right\} \tag{16}$$

$$\rho^{t+1} = \arg\min_{\rho, L_i} \left\|F_u\rho^t - d\right\|_2^2 + \beta\left\|\rho^t - \omega^{t+1} + m^t\right\|_2^2 \tag{17}$$

$$m^{t+1} = m^t + \mu\left(\rho^{t+1} - \omega^{t+1}\right) \tag{18}$$

The solution of nuclear norm in equation (16) belongs to low-rank matrix filling problem. In classic algorithm, it can be solved by singular value decomposition and singular value threshold shrinkage, namely:

$$\begin{cases} (U, \Sigma, V) = svd(X) \\ \hat{\Sigma} = S_\tau(\Sigma) \end{cases} \tag{19}$$

To improve the performance of singular value threshold shrinkage, a dynamic threshold shrinkage is applied to help reduce the error, namely:

$$S_{\omega,\tau}(\Sigma_{ii}) = \max(\Sigma_{ii} - \tau\omega_i, 0) \tag{20}$$

In order to reduce the computational complexity of the algorithm, the solution of the equation (17) sub-problem is solved by relocating the similar block position once every J iteration instread of performing similar block groups in each iteration.

To estimate the efficiency of the proposed method, called CS-DNLR, a series of exoeriments has been proceed. Here, an example of reconstruction MR brain image result is introduced. This MR image data was a T1 weighted MR image and was accquired from a 3 Tesla MRI Equipment with these parameters: FSE Sequence encoding, 384×324 image resolution, TR=1,000 ms, TE=0.84ms, slice thickness 5mm, see Fig. 1 (a). And the sampling mask is also shown in Fig. 1 (b).

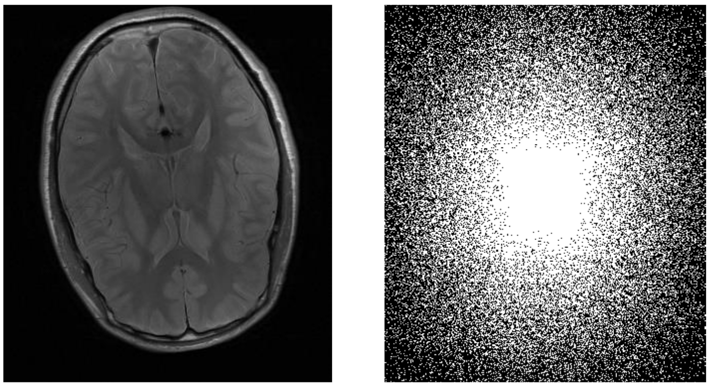

(a) orignal image (b) sampling mask

Fig. 1 orignal MR brain image and sampling mask

Two other methods is introduced, respectively CS-WL1[13] and CS-DNLR[14]. The experiment results is shown as in Fig. 2. It turns out that CS-DNLR reconstruction result is better than other two metods, both in geometric structure and in texture detail. And the detail performance comparison is shown as in Table 1.

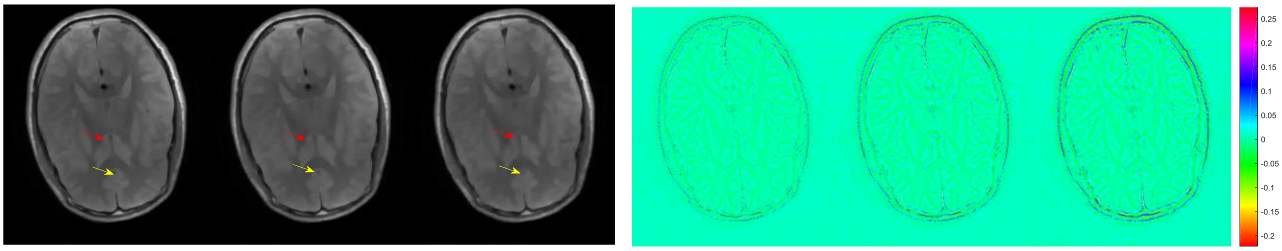

(a) CS-WLl result (b) CS-WLl residual error (-0.2~0.25)

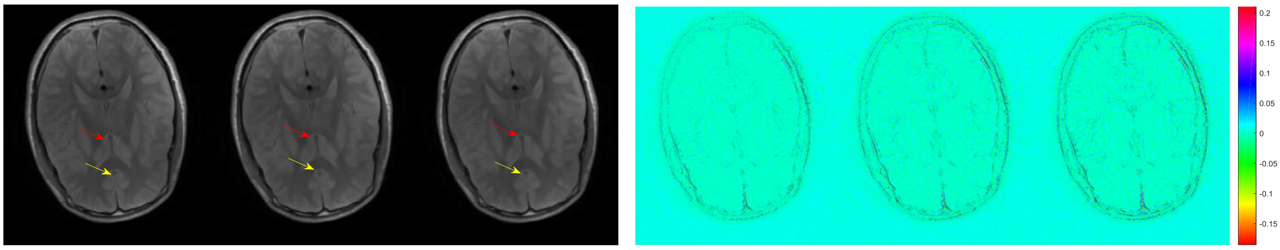

(c) CS-TV result (d) CS-TV residual error (-0.15~0.2)

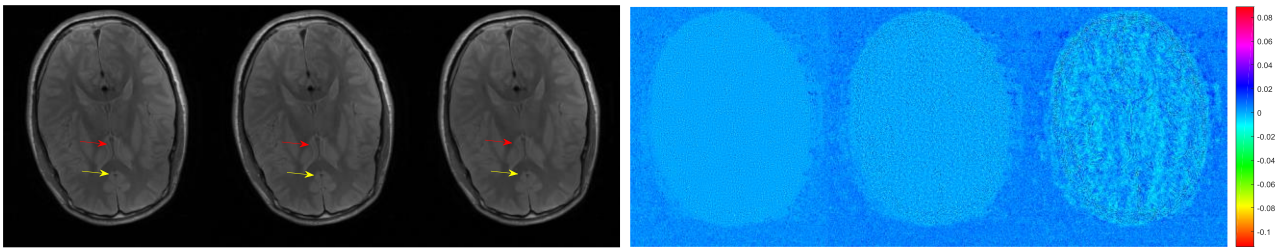

(e) CS-DNLR result (f) CS-DNLR residual error (-0.1~0.08)

Fig. 1 Reconstruction comparison of MR brain image by Three Methods

Table 1 Comparison of experiment results with RE PSNR and SSIM

Method	Sampling Speed	Relative Error/%	PSNR/dB	SSIM
CS-WLl	2	8.25	38.10	0.796
CS-TV	3	9.57	37.43	0.790
CS-DNLR	5	11.01	36.83	0.778
CS-WLl	2	6.65	39.81	0.841
CS-TV	3	7.27	39.29	0.836

CS-DNLR	5	7.83	38.83	0.833
CS-WLl	2	3.64	44.51	0.963
CS-TV	3	4.47	42.37	0.938
CS-DNLR	5	5.65	39.20	0.920

4. Conclusion

In this paper, an improved reconstruction algorithm based on the nonlocal low-rank matrix is applied to the study of MR image reconstruction. Unlike general methods, the low-rank dictionary is used as a regularization for compressed sensing optimization, and a dynamic threshold shrinkage method is used to update Lagrange multipliers instead of using fixed parameters. Experiment results show that this method significantly improves the quality of reconstructed images, and overcomes the shortcomings of the common models. The CS-DNLR algorithm can not only effectively retain the geometric structure and texture detail in MR images, but also eliminates the ladder artifact, which is such important for the clinical.

References

[1] Liang Z P, Lauterbur P C. Principles of magnetic resonance imaging: a signal processing perspective[M]. SPIE Optical Engineering Press, 2000.

[2] Coakley F V, Lopoo J B, Lu Y, et al. Normal and hypoplastic fetal lungs: volumetric assessment with prenatal single-shot rapid acquisition with relaxation enhancement MR imaging[J]. Radiology, 2000, 216(1): 107-111

[3] Yokoo T, Bydder M, Hamilton G, et al. Nonalcoholic fatty liver disease: diagnostic and fat-grading accuracy of low-flip-angle multiecho gradient-recalled-echo MR imaging at 1.5 T[J]. Radiology, 2009, 251(1): 67-76C. Li, W.Q. Yin, X.B. Feng, et al. Brushless DC motor stepless speed regulation system based on fuzzy adaptive PI controller, Journal of Mechanical & Electrical Engineering, vol. 29 (2012), 49-52.

[4] Pruessmann K P. Encoding and reconstruction in parallel MRI[J]. NMR in Biomedicine, 2006, 19(3): 288-299.

[5] Donoho D L. Compressed sensing[J]. IEEE Transactions on information theory, 2006, 52(4): 1289-1306

[6] Lustig M, Donoho D L, Santos J M, et al. Compressed sensing MRI[J]. IEEE signal processing magazine, 2008, 25(2): 72-82.

[7] Candès E J, Romberg J, Tao T. Robust uncertainty principles: Exact signal reconstruction from highly incomplete frequency information[J]. IEEE Transactions on information theory, 2006, 52(2): 489-509.

[8] Lustig M, Donoho D, Pauly J M. Sparse MRI: The application of compressed sensing for rapid MR imaging[J]. Magnetic resonance in medicine, 2007, 58(6): 1182-1195.

[9] Peng X, Du H Q, Lam F, et al. Reference-driven MR image reconstruction with sparsity and support constraints[C]//Biomedical Imaging: From Nano to Macro, 2011 IEEE International Symposium on. IEEE, 2011: 89-92.

[10] Hu L, Zhou J, Shi Z, et al. A fast and accurate reconstruction algorithm for compressed sensing of complex sinusoids[J]. IEEE Transactions on Signal Processing, 2013, 61(22): 5744-5754.

[11] Buades A, Coll B, Morel J M. A Review of Image Denoising Algorithms, with a New One[J]. Siam Journal on Multiscale Modeling & Simulation, 2006, 4(2):490—530.

[12] Candès E J, Recht B. Exact Matrix Completion via Convex Optimization[J]. Foundations of Computational Mathematics, 2009, 9(6):717.

[13] Tobisch A, Stöcker T, Groeschel S, et al. Iteratively reweighted L1-fitting for model-independent outlier removal and regularization in diffusion MRI[C]//Biomedical Imaging (ISBI), 2016 IEEE 13th International Symposium on. IEEE, 2016: 911-914.

[14] Hagtvedt T, Seierstad T, Lund K V, et al. Diffusion-weighted MRI compared to FDG PET/CT for assessment of early treatment response in lymphoma[J]. Acta Radiologica, 2015, 56(2): 152-158.